



## Spin-orbit-coupled depairing of a dipolar biexciton superfluid

S. V. Andreev 

National Research Center “Kurchatov Institute,” B. P. Konstantinov Petersburg Nuclear Physics Institute, Gatchina 188300, Russia

 (Received 27 July 2020; revised 21 April 2021; accepted 21 April 2021; published 5 May 2021)

We consider quantum phase transitions in a system of bright dipolar excitons which can form bound pairs (dipolar biexcitons). The biexciton energy is tuned from negative to positive values through the scattering threshold. At sufficiently large density an exciton superfluid transforms into a superfluid of biexcitons. With the average relative momenta of excitons in the pairs being beyond the light cone, the transition is accompanied by a reduction of the photoluminescence intensity. Effective magnetic fields due to the long-range exchange splitting of exciton states shift the position of the gap in the elementary excitation spectrum to a circle of degenerate minima in the  $\mathbf{k}$  space. Closing the gap results in the formation of exciton stripes polarized linearly along the direction of their translational symmetry. In the biexciton energy vs density phase diagram the novel phase intervenes between the dark biexciton and radiative exciton superfluids. We conclude that formation of a BCS-like biexciton condensate induces correlated alignment of the effective magnetic fields and excitonic spins. We outline important differences in the predicted mechanism from the phenomenon of spin-orbit-coupled Bose-Einstein condensation.

DOI: [10.1103/PhysRevB.103.184503](https://doi.org/10.1103/PhysRevB.103.184503)

### I. INTRODUCTION

Excitonic molecules (biexcitons) have attracted great interest since the very beginning of the quest for Bose-Einstein condensation (BEC) in solids [1]. The concept of a biexciton is an extension of the analogy between an exciton and a hydrogen atom to the case of two quasiparticles: exchange of the constituent fermions in the spin-singlet configuration stabilizes a bound state of bosons [2–7]. At low temperatures a biexciton condensate should compete with a condensate of unpaired excitons [8].

With the advent of semiconductor technology, well-resolved biexciton lines have been observed in photoluminescence (PL) of quantum wells (QWs) [9–11] and, more recently, atomically thin layers of transition metal dichalcogenides (TMDs) [12–16]. Bilayer structures or wide single QWs subjected to a transverse electric field host dipolar excitons with long radiative lifetimes  $\tau$  and high cooling rates [15–26]. The inset in Fig. 1 shows schematically a pair of dipolar excitons each composed of an electron and a hole residing in spatially separated layers. A dipolar exciton possesses a permanent dipole moment oriented in the transverse direction (the  $z$  axis). In addition, it also has a pseudospin defined by  $z$  projections of the fermionic spins and valley indices. Among a great variety of excitonic species only the so-called bright excitons characterized by two possible pseudospin states ( $|\uparrow\rangle$  or  $|\downarrow\rangle$ ) may recombine, emitting a photon (right- or left-circularly polarized, respectively) [27]. The typical biexcitonic PL line corresponds to a bound state of two bright excitons with opposite spins (i.e.,  $|\uparrow\rangle$  and  $|\downarrow\rangle$ ).

For large separation between the layers dipolar repulsion prevents formation of biexcitons and favors excitonic BEC [28,29]. Before completely disappearing, however, a dipolar

biexciton has been predicted to transform into a resonance [30,31]. As opposed to a true bound state, the resonance may have a positive energy  $\varepsilon$  and a finite width  $\beta$  defined by tunneling of excitons under the dipolar potential barrier (Fig. 1). As one increases the density, a resonantly paired exciton superfluid (X) undergoes a quantum phase transition

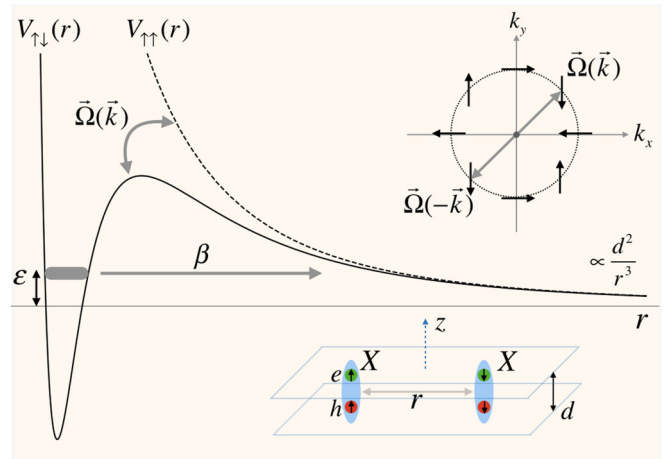


FIG. 1. Sketch of the two-body interaction potentials for excitons with parallel (dashed line) and antiparallel (solid line) spins. The latter features a biexciton resonance with energy  $\varepsilon$  and natural width  $\beta$  defined by tunneling of excitons under the barrier due to the dipolar repulsion. The inset in the top right corner shows orientations of the effective magnetic field  $\Omega(\mathbf{k})$  with respect to the exciton wave vector  $\mathbf{k}$ . The field  $\Omega(\mathbf{k})$  couples the  $|\uparrow\downarrow\rangle$  and  $|\uparrow\uparrow\rangle$  (or  $|\downarrow\downarrow\rangle$ ) scattering channels. The bottom inset shows a pair of dipolar excitons (X) formed of spatially separated electrons (e) and holes (h).

to a superfluid of biexcitons (XX). The dipolar biexcitons are stabilized in the media by mean-field repulsion, with single excitons occurring only as gapped elementary excitations of the superfluid [32].

Extended spatial and temporal coherence, which may be accessed by shift-interferometry measurements of the PL [18,19,26], is suppressed in the XX phase due to the relative motion of excitons within a molecule [30]. For the same reasons, one may expect suppression of the PL intensity: as the effective binding tightens, the excitons are extruded outside of the “light cone” [33]. The latter defines a circle of a radius  $q_0$  in two-dimensional (2D) momentum space, inside of which a bright exciton can recombine, emitting a photon [27]. Beyond the light cone the exciton dispersion acquires fine structure due to the long-range exchange interaction between the electron and the hole [34–37]. The effect of the long-range exchange on pairing of dipolar excitons is a challenging question which has not been addressed until now.

The exciton Hamiltonian accounting for the long-range exchange can be written as

$$\hat{H}_0 = \sum_{p, \sigma, \sigma' = \uparrow, \downarrow} [T_p \delta_{\sigma\sigma'} - \hbar \mathbf{\Omega}(p) \cdot \mathbf{S}_{\sigma\sigma'}] \hat{a}_{\sigma, p}^\dagger \hat{a}_{\sigma', p}, \quad (1)$$

where the first term  $T_p = \hbar^2 p^2 / 2m + \hbar v p / 2$  is modified kinetic energy and the second term has the form of interaction of the exciton pseudospin

$$\mathbf{S} = \frac{1}{2} (\sigma_x \mathbf{n}_x + \sigma_y \mathbf{n}_y + \sigma_z \mathbf{n}_z), \quad (2)$$

with the 2D effective magnetic field

$$\mathbf{\Omega}(p) = -v p (\mathbf{n}_x \cos 2\varphi + \mathbf{n}_y \sin 2\varphi). \quad (3)$$

Here  $\sigma_x, \sigma_y,$  and  $\sigma_z$  are the Pauli matrices,  $p$  and  $\varphi$  are the polar coordinates of the 2D wave vector of exciton translational motion  $\mathbf{p}$ , and

$$v = (\tau q_0)^{-1}. \quad (4)$$

By virtue of the symmetry with respect to the time reversal and bosonic nature of excitons, the magnetic field (3) is an even function of  $\mathbf{p}$  (Fig. 1).

The lower-energy eigenstate of (1) is a plane wave with its pseudospin

$$|\varphi\rangle = -e^{-i\varphi} |\uparrow\rangle + e^{i\varphi} |\downarrow\rangle \quad (5)$$

pointing in the direction of  $\mathbf{\Omega}(p)$ . Such pseudospin orientation corresponds to the exciton linear polarization lying in the structure plane and being transverse with respect to  $\mathbf{p}$ . The dispersion of the transverse exciton  $E_\perp(p) = \hbar^2 p^2 / 2m$  is split from the upper branch  $E_\parallel(p) = \hbar^2 p^2 / 2m + \Delta_{LT}(p)$  polarized along  $\mathbf{p}$  by the amount  $\Delta_{LT}(p) = \hbar v p$ , known as the longitudinal-transverse (LT) splitting [35–37].

In contrast to the single-particle dispersions in the presence of conventional spin-orbit (SO) coupling [38–43], the functions  $E_\perp(p)$  and  $E_\parallel(p)$  are *monotonous*. This excludes exotic phases predicted [44] and subsequently realized [45,46] in SO-coupled atomic Bose-Einstein condensates. Moreover, for dipolar excitons the exchange splitting is small due to

reduced overlap between the electron and hole wave functions [long exciton lifetime  $\tau$  in Eq. (4)]. Surprisingly, as we demonstrate in this paper, weak SO coupling of the type (1) may alter dramatically bosonic BCS-BEC phase transition. We show that in a dipolar biexciton superfluid the microscopic fields  $\mathbf{\Omega}(p)$  unify to produce a new efficient pair-breaking mechanism. The fields shift the position of the gap in the XX elementary excitation spectrum from  $\mathbf{p} = 0$  to a circle of rotonlike minima at  $|\mathbf{p}| = p_0$ . The value of  $p_0$  is defined by the balance between the kinetic energy and interaction of the exciton spin with a *collective* exchange field. As one closes the new gap (e.g., by decreasing the exciton density  $n$ ), the fields  $\mathbf{\Omega}(p)$  spontaneously align all in the same direction, and depairing of the biexciton superfluid occurs in a superposition of  $\mathbf{p}_0$  and  $-\mathbf{p}_0$  plane-wave excitonic condensates spin polarized along  $\mathbf{\Omega}(p_0)$  [Eq. (16)]. We denote this phase as  $\mathbf{\Omega}$ -X-XX. The polarized excitonic stripes in the  $\mathbf{\Omega}$ -X-XX phase originate from SO-coupled depairing of a BCS-like condensate of loosely bound excitonic molecules. The wave vector  $p_0$  [Eq. (14)] has its maximum value at the  $\mathbf{\Omega}$ -XX/ $\mathbf{\Omega}$ -X-XX phase transition boundary and approaches the light cone  $q_0$  as one further decreases the density. At that point the  $\mathbf{\Omega}$ -X-XX phase turns into the radiative exciton superfluid X.

## II. THE MODEL

The full many-body Hamiltonian reads  $\hat{H} = \hat{H}_0 + \hat{V}$ , where

$$\hat{V} = \frac{1}{2S} \sum_{\mathbf{p}_1, \mathbf{p}_2, \mathbf{q}, \sigma, \sigma'} \hat{a}_{\sigma, \mathbf{p}_1 + \mathbf{q}}^\dagger \hat{a}_{\sigma', \mathbf{p}_2 - \mathbf{q}}^\dagger V_{\sigma\sigma'}(\mathbf{q}) \hat{a}_{\sigma, \mathbf{p}_1} \hat{a}_{\sigma', \mathbf{p}_2} \quad (6)$$

is the two-body interaction in a binary mixture of interacting bosons and  $V_{\sigma\sigma'}(\mathbf{q}) = \int e^{-i\mathbf{q}\mathbf{r}} V_{\sigma\sigma'}(\mathbf{r}) d\mathbf{r}$ . The potentials  $V_{\uparrow\uparrow}(\mathbf{r})$  and  $V_{\downarrow\downarrow}(\mathbf{r})$  are repulsive at all distances, whereas  $V_{\uparrow\downarrow}(\mathbf{r})$  features a resonance, characterized by its energy  $\varepsilon$  and width  $\beta$  (Fig. 1). The resonance emerges from a true bound state as the distance between the electron-hole layers  $d$  crosses the threshold value on the order of the electron Bohr radius  $a_e = \hbar^2 \kappa / m_e e^2$  [31]. We note parenthetically that the generic potential  $V_{\uparrow\downarrow}(\mathbf{r})$  can be employed to model resonant pairing in a large variety of fermionic [47–49] and bosonic [50–52] systems. Throughout this paper we assume  $\varepsilon \gg \beta$ .

For a typical MoS<sub>2</sub>-based heterostructure the momentum cutoff imposed by the light cone corresponds to a pair energy on the order of  $\varepsilon \sim 10 \mu\text{eV}$ . At the X-XX transition one has  $\varepsilon \sim \mu$ . The chemical potential of a 2D exciton condensate can be estimated by using the transcendental formula  $\mu = 4\pi / \ln(E_a / 2\mu) \hbar^2 n / m$  [53], where  $m$  is the exciton mass and  $E_a = \hbar^2 / m a^2$ , with  $a$  being on the order of the exciton Bohr radius  $a_X$ . We thus obtain  $n_{\min} \sim 10^{10} \text{ cm}^{-2}$  for the reference exciton density separating the radiative and dark regimes. At such densities the system shares analogies with gaseous atomic superfluids [54,55]. For  $\varepsilon > 0$  the long-range dipolar repulsion between the excitons may induce coherent crystallization of a resonantly paired superfluid via the roton instability [31,56] (also predicted for pancake atomic condensates [57]). Possible competition of the  $\mathbf{\Omega}$ -X-XX phase with the dipolar supersolid will be the subject of our future work. As we shall see, the  $\mathbf{\Omega}$ -X-XX

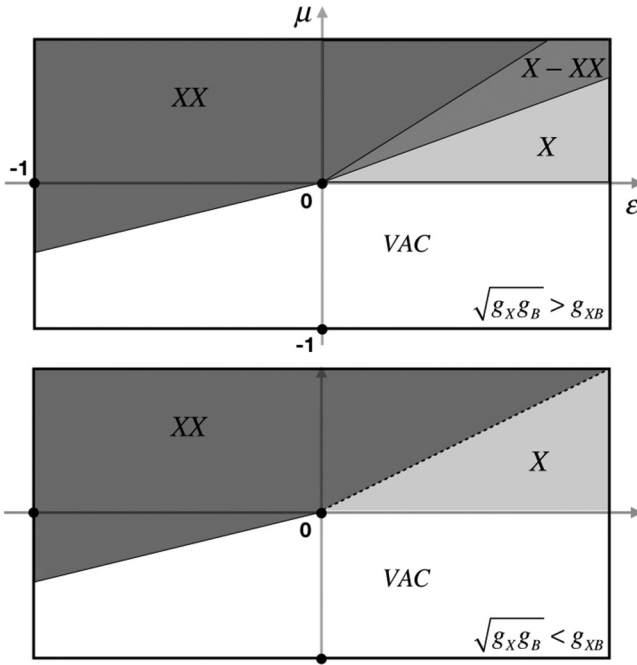


FIG. 2. Sketches of the two possible phase diagrams of a resonantly paired exciton condensate with  $\beta = 0$  in the radiative regime ( $|\varepsilon| < 1$  in units of  $\hbar^2 q_0^2/m$ ). Depending on whether  $\sqrt{g_X g_B} < g_{XB}$  or  $\sqrt{g_X g_B} > g_{XB}$ , the transition to the biexciton phase (XX) at  $\varepsilon > 0$  may be either of the first or the second kind, respectively. The second-order transition occurs via an intermediate mixed phase (X-XX), where a fraction of biexcitons is dissolved in the exciton superfluid (X).

phase penetrates also into the region  $\varepsilon < 0$ , where the potential  $V_{\uparrow\downarrow}(\mathbf{r})$  is characterized by vanishingly small scattering amplitude and the dipolar crystallization is prevented by the background repulsion in the other two channels. We expect the corresponding domain in the phase diagram (see Fig. 3 below) to be the most suitable for neat observation of the phenomena predicted in the present work.

As one increases  $\varepsilon$  toward its upper positive bound (presumably on the order of the biexciton binding energy, 10 meV [12]), the characteristic exciton density approaches  $n_{\max} \sim 10^{12} \text{ cm}^{-2}$ . Although it is presently unclear whether the resonance remains narrow in this limit, working with such a dense quasicondensate characterized by large  $\mu$  represents several advantages. First, such density corresponds to the relatively high Berezinskii-Kosterlitz-Thouless (BKT) transition temperature  $T_{\text{BKT}} \sim 10 \text{ K}$  [58]. Second, the disorder present in moderate-quality samples is screened by the repulsive interactions [59]. At the same time, since we are concerned with  $d \sim a_e$ , the dipolar repulsion is not strong enough to crystallize the superfluid [58,60–62].

### III. RADIATIVE REGIME

It is instructive to discuss first the infinitely narrow resonance limit ( $\beta = 0$ ) of the radiative dilute X and XX phases. The exchange splitting is absent, and we may describe the ground state by the following system of Gross-Pitaevskii

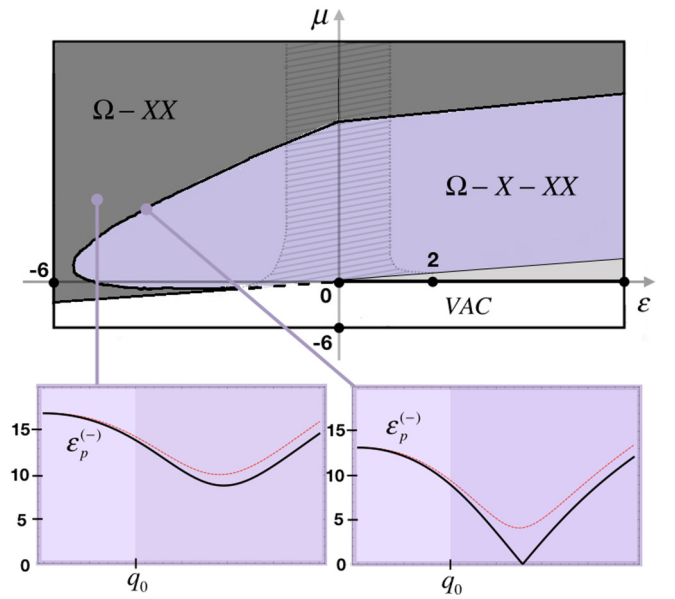


FIG. 3. The phase diagram of a paired exciton condensate with spin-orbit coupling. We adopt units of  $\hbar^2 q_0^2/m$ , where  $q_0$  corresponds to the boundary of the light cone. The insets show exemplary spectra of elementary excitations in the biexciton phase [ $\Omega$ -XX, dark gray; Eq. (13)]. Red dashed lines account for the exchange term in the kinetic energy in Eq. (11). Closure of the rotonlike gap defines a second-order phase boundary with a new  $\Omega$ -X-XX phase (magenta) characterized by smectic order and transverse linear polarization of excitons [Eq. (16)]. The hatch in the vicinity of  $|\varepsilon| = 0$  marks the region where the magnitude of  $\mathbf{p}_0$  becomes inferior to  $q_0$ . In the region  $\varepsilon > 0$  the  $\mu = \varepsilon/2$  line marks a boundary with the radiative exciton superfluid X (light gray). We have used the parameters typical for a MoS<sub>2</sub> homobilayer. More details can be found in Appendixes B and C.

equations:

$$\begin{aligned} 2\mu\Psi_B &= (\varepsilon + g_B|\Psi_B|^2 + g_{\uparrow B}|\Psi_{\uparrow}|^2 + g_{\downarrow B}|\Psi_{\downarrow}|^2)\Psi_B, \\ \mu\Psi_{\sigma} &= (g_{\sigma\uparrow}|\Psi_{\uparrow}|^2 + g_{\sigma\downarrow}|\Psi_{\downarrow}|^2 + g_{\sigma B}|\Psi_B|^2)\Psi_{\sigma}, \end{aligned} \quad (7)$$

where  $\Psi_{\sigma}$  and  $\Psi_B$  stand for the exciton and biexciton order parameters, respectively, and  $\sigma = \{\uparrow, \downarrow\}$ . One has  $2|\Psi_B|^2 + |\Psi_{\uparrow}|^2 + |\Psi_{\downarrow}|^2 = n$ . The effective interactions  $g_{\sigma\sigma'}$  account for both the short-range part and the dipolar tail of the bare potentials  $V_{\sigma\sigma'}(\mathbf{r})$  [53]. We omit the momentum-dependent correction due to the dipolar tail assuming that this correction is small compared to the mean contact part. This way, we exclude the dipolar-supersolid scenario from the consideration [30,31,61]. The phenomenologically introduced potentials  $g_{\sigma B}$  and  $g_B$  are positive constants on the order of  $g_{\sigma\sigma'}$ . By symmetry, we assume  $g_{\uparrow\uparrow} = g_{\downarrow\downarrow} \equiv g_X$ ,  $g_{\uparrow B} = g_{\downarrow B} \equiv g_{XB}$ , and  $|\Psi_{\uparrow}| = |\Psi_{\downarrow}|$ . Miscibility of excitons with different spins requires  $g_{\uparrow\downarrow} < g_X$ . We may let  $g_{\uparrow\downarrow} \equiv 0$  without loss of generality.

Solving the system (7) yields the phase diagram shown in Fig. 2. The region  $\varepsilon < 0$  corresponds to a true bound state. Condensation here occurs directly into the XX phase, with the condensate density growing as  $|\Psi_B|^2 = (2\mu - \varepsilon)/g_B$ .

Signatures of such a second-order transition in the exciton thermodynamics were reported in Ref. [10].

In the region  $\varepsilon > 0$  the condensation starts in the X phase at the second-order phase transition line  $\mu = 0$ . Depending on whether  $\sqrt{g_X g_B} < g_{XB}$  or  $\sqrt{g_X g_B} > g_{XB}$ , the subsequent transition to the XX phase may be either of the first or the second kind, respectively. The second-order transition occurs via an intermediate mixed phase (X-XX), where a fraction of biexcitons is dissolved in the X superfluid. The X/X-XX second-order boundary is located at  $\mu = \varepsilon/(2 - g_{XB}/g_X)$ . As one increases the chemical potential  $\mu$ , the biexciton fraction grows, and at

$$\mu = \varepsilon/(2 - g_B/g_{XB}) \quad (8)$$

the X-XX mixture continuously turns into the XX superfluid.

Assuming that the effective interactions are inversely proportional to the reduced mass of the particle relative motion

$$\begin{aligned} \hat{H}_\Omega = E_B + \sum_{p,\sigma=\uparrow,\downarrow} \xi_p \hat{a}_{\sigma,p}^\dagger \hat{a}_{\sigma,p} + \frac{g_X}{2S} \sum_{\mathbf{p}_1, \mathbf{p}_2, \mathbf{q}, \sigma} \hat{a}_{\sigma, \mathbf{p}_1 + \mathbf{q}}^\dagger \hat{a}_{\sigma, \mathbf{p}_2 - \mathbf{q}}^\dagger \hat{a}_{\sigma, \mathbf{p}_1} \hat{a}_{\sigma, \mathbf{p}_2} \\ - \sum_{\mathbf{p}} \hbar[\boldsymbol{\Omega}_B(\mathbf{p}) + \boldsymbol{\Omega}_B(-\mathbf{p})] \cdot (\mathbf{S}_{\uparrow\downarrow} \hat{a}_{\uparrow, \mathbf{p}}^\dagger \hat{a}_{\uparrow, -\mathbf{p}}^\dagger + \mathbf{S}_{\downarrow\uparrow} \hat{a}_{\downarrow, \mathbf{p}}^\dagger \hat{a}_{\downarrow, -\mathbf{p}}^\dagger) - \sqrt{\frac{\hbar^2 n_B \beta}{2\pi m}} \sum_{\mathbf{p}} \hat{a}_{\uparrow, \mathbf{p}}^\dagger \hat{a}_{\downarrow, -\mathbf{p}}^\dagger + \text{H.c.} \end{aligned} \quad (9)$$

Here

$$E_B = (\varepsilon - 2\mu)N_B + \frac{g_B N_B^2}{2S} \quad (10)$$

is the (grand canonical) energy of the molecular condensate and

$$\xi_p = \frac{\hbar^2 p^2}{2m} + \frac{\hbar v p}{2} + g_{XB} |\Psi_B|^2 - \mu \quad (11)$$

is the energy of unpaired excitons in the mean-field potential produced by the molecules. The occupation number  $N_B$  is related to the molecular order parameter by  $|\Psi_B|^2 = N_B/S \equiv n_B$ . The last term accounts for the natural width  $\beta$  of the resonance due to dissociation through the dipolar potential barrier [31].

The molecular condensate unifies the microscopic exchange fields (3) into a macroscopic field

$$\boldsymbol{\Omega}_B(\mathbf{p}) = \sqrt{N_B} \phi_p \boldsymbol{\Omega}(\mathbf{p}), \quad (12)$$

flipping the spins of unpaired excitons. In the relevant limit of small exchange splitting of the single-particle states the wave function of the exciton relative motion  $\phi_p$  can be obtained from the one-channel Schrodinger equation (A7). By virtue of the spherical symmetry of  $V_{\uparrow\downarrow}(\mathbf{r})$  the phase of  $\phi_p$  does not depend on  $\mathbf{p}$ . Our choice of the sign of the last term in (9) corresponds to this phase being zero.

#### A. The pair-breaking excitation spectrum

In the SO-coupled XX phase (which from now on we shall call  $\boldsymbol{\Omega}$ -XX) one may neglect the interaction between unpaired excitons [the third term in the Hamiltonian (9)]. The standard Bogoliubov–de Gennes approach then yields the spectrum of

[53], one may conclude that the transition should be first order (dashed line in Fig. 2). This result is modified dramatically by the long-range exchange, as we shall see below.

#### IV. SO-COUPLED DEPAIRING OF A DIPOLAR BIEXCITON SUPERFLUID

We now consider  $|\varepsilon| \gg \hbar^2 q_0^2/m$ . In this case the excitons are subjected to the exchange fields [Eq. (1)]. We notice that at the two-body level the exchange field  $\boldsymbol{\Omega}(\mathbf{p})$  couples the  $|\uparrow\uparrow\rangle$  and  $|\downarrow\downarrow\rangle$  repulsive scattering channels to the  $|\uparrow\downarrow\rangle$  pairing channel. One may also say that the exchange destroys a biexciton by flipping the spin of either of the two excitons. This motivates us to consider the following BCS-like Hamiltonian (rigorous derivation is given in Appendix A):

elementary excitations

$$\varepsilon_p^{(\pm)} = \sqrt{\xi_p^2 - \left[ \sqrt{\frac{\hbar^2 n_B \beta}{2\pi m}} \pm 2|\hbar \boldsymbol{\Omega}_B^{(s)}(\mathbf{p}) \cdot \mathbf{S}_{\uparrow\downarrow}| \right]^2}, \quad (13)$$

where we have introduced the short-hand notation  $\boldsymbol{\Omega}_B^{(s)}(\mathbf{p}) \equiv \boldsymbol{\Omega}_B(\mathbf{p}) + \boldsymbol{\Omega}_B(-\mathbf{p})$ . To develop a feel for the effect of the exchange term on the biexciton superfluid we let  $\beta \rightarrow 0$ . In this limit, the spectrum (13) consists of a single branch. The gap at  $\mathbf{p} = 0$  is given by  $\xi_0$  and would close precisely at the second-order phase transition boundaries identified in the previous section. This happens, however, only for sufficiently small exciton dipole moment. As the bound state approaches the scattering threshold, the collective exchange field becomes increasingly large due to growth of the molecular radius  $a_B = \sqrt{\hbar^2/m|\varepsilon|}$ . Thus, assuming  $pa_B \ll 1$ , one has  $\phi_p = \sqrt{4\pi a_B^2/S}$ , which upon substitution into Eq. (12) yields  $\boldsymbol{\Omega}_B(\mathbf{p}) = \nu p \sqrt{4\pi n_B a_B^2}$ . For  $a_B \gg a_X$  the spin-flip term  $|\hbar \boldsymbol{\Omega}_B(\mathbf{p}) \cdot \mathbf{S}_{\uparrow\downarrow}|$  may outweigh the exchange contribution to the kinetic energy [the second term in Eq. (11)] already in the dilute regime  $na_X \ll 1$ . Depairing of excitons at finite momentum accompanied by alignment of their spins along  $\boldsymbol{\Omega}_B(\mathbf{p})$  then costs less energy than  $\xi_0$ : the gap shifts to a circle of rotonlike minima at  $|\mathbf{p}| = p_0$ . The magnitude of  $p_0$  is defined by the balance between the interaction of the exciton spin with  $\boldsymbol{\Omega}_B(\mathbf{p})$  and the massive part of the kinetic energy [the first term in Eq. (11)]. The divergent behavior of  $\boldsymbol{\Omega}_B(\mathbf{p})$  at  $|\varepsilon| \rightarrow 0$  is regularized by accounting for the full momentum dependence of the wave function  $\phi_p$  (Appendix B). The results are presented in Fig. 3. The insets show exemplary spectra at two points on the phase diagram. On the  $\varepsilon > 0$  side

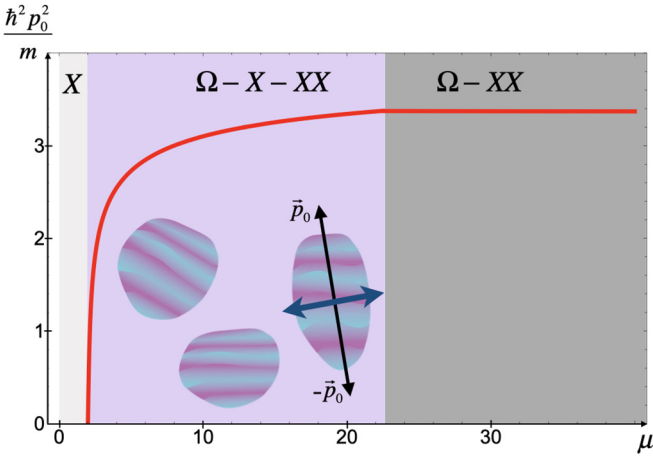


FIG. 4. The magnitude of the wave vector  $\mathbf{p}_0$  as a function of the chemical potential  $\mu$  along the line  $\varepsilon = 4$  of the phase diagram shown in Fig. 3. Units of  $\hbar^2 q_0^2/m$  are used. In the  $\Omega$ -XX phase (dark gray area) the magnitude of  $\mathbf{p}_0$  corresponds to the rotonlike minimum in the pair-breaking excitation spectrum. In the  $\Omega$ -X-XX phase (magenta) the wave vector  $\mathbf{p}_0$  defines the period and the local orientation of the exciton stripes pictured schematically in the inset. The transverse arrow depicts the linear polarization of excitons. The magnitude of  $\mathbf{p}_0$  here is a solution of Eq. (14).

the observed behavior extends far beyond the light-cone area (hatched): the strength of the exchange field  $\Omega_B(\mathbf{p})$  at decreasing  $a_B$  is maintained by the increase of the biexciton density. Closure of the new gap defines a second-order transition to an exotic phase, whose nature will be elucidated below.

### B. The $\Omega$ -X-XX phase

In contrast to the X-XX mixture discussed for the radiative regime in Sec. III, the X component of the  $\Omega$ -X-XX phase represents a superposition of plane-wave condensates. The corresponding mean-field energy density can be obtained from Eq. (9) by substituting  $\hat{a}_{\sigma,p}/\sqrt{S} \rightarrow \Psi_{\sigma,\pm q}\delta_{p,\pm q}$ , where  $\delta_{p,q} = 1$  for  $\mathbf{p} = \mathbf{q}$  and  $\delta_{p,q} = 0$  otherwise. Canonical transformation of the resulting quadratic form shows that the minimum of the energy is achieved by the choice  $\Psi_{\sigma,q} = \Psi_{-\sigma,-q}^*$  and  $\Psi_{\uparrow,q} = -e^{-2i\varphi}\Psi_{\downarrow,q}$ , with  $|\mathbf{q}| = p_0$  being the solution of

$$\frac{\partial}{\partial q} |\Omega_B^{(s)}(\mathbf{q}) \cdot \mathbf{S}_{\uparrow\downarrow}| - \frac{\hbar q}{2m} = \frac{\nu}{4} \quad (14)$$

and  $|\Psi_{\uparrow,\pm q}| = |\Psi_{\downarrow,\pm q}| \equiv |\Psi_X|$ , where

$$|\Psi_X| = \sqrt{\frac{\sqrt{\frac{\hbar^2 n_B \beta}{2\pi m}} + 2|\hbar\Omega_B^{(s)}(\mathbf{p}_0) \cdot \mathbf{S}_{\uparrow\downarrow}| - \xi_{p_0}}{8g_X}}. \quad (15)$$

The exciton order parameter

$$\Psi_X(\mathbf{r}) = i|\Psi_X| \sin(\mathbf{p}_0 \cdot \mathbf{r} + \theta - \varphi_0) |\varphi_0\rangle \quad (16)$$

has a periodical spatial structure and spin polarization given by Eq. (5) with  $\varphi \equiv \varphi_0$ . Here  $\varphi_0$  is the polar angle of  $\mathbf{p}_0$ . The magnitude of  $\mathbf{p}_0$  is on the order of  $a_B^{-1}$  at the  $\Omega$ -XX/ $\Omega$ -X-XX phase boundary and rapidly decreases as one lowers the chemical potential (Fig. 4). We tentatively associate such behavior

with expansion of the size of bosonic ‘‘Cooper pairs’’ constituting the XX component.

The phase  $\theta = \text{Arg}(\Psi_{\uparrow,q})$  is due to the broken  $U_N(1)$  symmetry associated with conservation of the total number of particles  $N = N_{\uparrow} + N_{\downarrow} + 2N_B$  (neither  $N_{\uparrow} + N_{\downarrow}$  nor  $N_{\uparrow} - N_{\downarrow}$  is conserved separately in our resonantly paired model with SO coupling). In addition to the gauge symmetry, the exciton density wave (16) breaks rotational  $O(2)$  and translational  $T_{p_0}$  symmetries, similar to the smectic phase of liquid crystals. Orientational ordering is accompanied by alignment of the microscopic magnetic fields  $\Omega(\mathbf{p}_0)$  according to the diagram shown in the inset of Fig. 1. These add up with the molecular field  $\Omega_B(\mathbf{p}_0)$  to induce the macroscopic spin texture  $\mathcal{S}(\mathbf{r}) = |\Psi_X|^2 \langle \varphi_0 | \mathbf{S} | \varphi_0 \rangle \sin^2(\mathbf{p}_0 \cdot \mathbf{r} + \theta - \varphi_0)$ .

The  $\Omega$ -X-XX phase has two Goldstone modes,  $\varphi_0$  and  $\theta$ , the latter standing simultaneously for smectic phonons in the exciton order parameter (16) and for the superfluid phase of the BCS-like biexcitonic component. The transition from this phase to the normal state thus falls into the  $O(3)$  universality class and is expected to be smeared by fluctuations [63,64]. At  $T > 0$  the density modulations would be destroyed, whereas the orientational order would persist in domains defined by thermal activation of dislocations [65]. A possible remedy is to break explicitly either of the two continuous symmetries: application of an external (electric or magnetic) field in the structure plane or injecting the pair coherence into the system by light would stabilize the new phase up to the standard BKT point.

Smearing of the stripes by quantum and thermal fluctuations should produce a small fraction of polarized excitons inside the light cone. This would produce a weak PL signal polarized linearly along the stripes. The crystalline order then should be signaled by the appearance of a higher-energy ‘‘umklapp’’ emission blueshifted by  $\hbar^2 p_0^2/2m$ . As one reduces the molecular fraction  $N_B$ , the magnitude of  $\mathbf{p}_0$  [Eq. (14)] approaches the light cone. At that point the  $\Omega$ -X-XX phase merges with the radiative exciton condensate X. Detailed investigation of this latter phase transition is outside the scope of the present study and will be given elsewhere.

### C. The role of the finite natural width $\beta$ of the resonance

Before we conclude, let us briefly comment on the role of the natural width  $\beta$  of the discrete biexciton level  $\varepsilon$ . At first glance, the assumption  $\varepsilon \gg \beta$  might be safely replaced by  $\beta = 0$ . This indeed provides a correct understanding of the impact of the exchange interaction on the elementary excitations and the phase diagram of a dipolar biexciton superfluid, as exemplified by Figs. 3 and 4. The necessity of keeping finite  $\beta$  stems from the symmetry considerations given in Sec. IV B. In fact, the tunneling of excitons under the dipolar potential barrier locks the relative phase between the X and XX components, thus reducing the total number of symmetries to be broken spontaneously. This makes possible the existence of disordered domains of the  $\Omega$ -X-XX phase at  $T > 0$  (schematically illustrated in the inset of Fig. 4). In the considerations given in Secs. IV A and IV B, such a reduction of symmetry manifests itself as lifting of the degeneracy of the excitation spectrum and of the ground state, respectively.

In the radiative regime, the phase diagram accounting for the finite  $\beta$  was worked out in Ref. [30]. By comparing that result with the diagram shown in Fig. 3, one may conclude that the latter will remain unchanged unless the boundary of the radiative X-XX phase bulges beyond the corresponding  $\Omega$ -X-XX boundary. In the region  $\varepsilon < 0$  broadening of the level may be induced by a constant contribution to the effective magnetic field acting on the exciton spin (e.g., by application of an external in-plane magnetic field). Here it may transform the segment of the line separating the  $\Omega$ -X-XX phase from the vacuum into a first-order boundary (provisionally marked by the dashed line in Fig. 3) [30].

Finally, we notice that part of our findings remains valid also in the limit of a broad resonance ( $\beta \gg \varepsilon$ ). The description involving the last term in Eq. (9) here does not apply. In all equations one should let  $\beta \equiv 0$  identically and consider only the region of a true bound state  $\varepsilon < 0$ .

## V. CONCLUSIONS AND OUTLOOK

Our consideration reveals that the molecular coherence at the BCS-BEC phase transition induces spontaneous alignment of (pseudo)spins and effective magnetic fields associated with the constituent bosons. In contrast to the phenomenon of SO-coupled BEC [41–46], this genuinely many-body effect does not require the presence of a finite-momentum minimum in the single-particle dispersion. The effect is suppressed on the BEC side of the transition by the mean-field repulsive interactions. A rotonlike feature in the pair-breaking excitation spectrum of the molecular BEC may be considered a precursor of the effect.

The proposed setting of bright dipolar excitons in TMDs and QWs provides the neatest demonstration of the phenomena due to smallness of the exchange splitting of the single-exciton states and monotonous character of their dispersions. However, our finding goes far beyond this particular scenario. First, our idea applies immediately to microcavity polaritons, where even SO coupling appears naturally due to both photonic and excitonic TE-TM splittings [66–68]. A polariton gas possessing the required pair correlations may be generated by using an appropriate excitation source (e.g., a radiative biexcitonic condensate XX). Second, bosonic BCS-BEC transition was recently demonstrated in ultracold atoms [69], revitalizing the subject [50–52]. These achievements together with the progress in simulation of SO coupling in neutral atoms [45,46,70,71] look promising for atomistic realization of the model considered in our work.

## ACKNOWLEDGMENTS

The author acknowledges the support from the Russian Science Foundation (Grant No. 18-72-00013).

## APPENDIX A: DERIVATION OF THE SO-COUPLED TERM IN THE BCS-LIKE BOSONIC HAMILTONIAN

In order to derive the SO-coupled term appearing in the BCS-like Hamiltonian presented in the main text, we first

consider single-particle Hamiltonians of the form

$$\hat{H}_i = \frac{\hbar^2}{2} \begin{pmatrix} m_*^{-1} \hat{\mathbf{k}}_i^2 & m_{\text{LT}}^{-1} \hat{\mathbf{k}}_{-i}^2 \\ m_{\text{LT}}^{-1} \hat{\mathbf{k}}_{+i}^2 & m_*^{-1} \hat{\mathbf{k}}_i^2 \end{pmatrix}, \quad (\text{A1})$$

which possess the useful property

$$\begin{aligned} \hat{H}_1 + \hat{H}_2 &= \frac{\hbar^2}{4} \begin{pmatrix} m_*^{-1} \hat{\mathbf{K}}^2 & m_{\text{LT}}^{-1} \hat{\mathbf{K}}^2 \\ m_{\text{LT}}^{-1} \hat{\mathbf{K}}_+^2 & m_*^{-1} \hat{\mathbf{K}}^2 \end{pmatrix} + \hbar^2 \begin{pmatrix} m_*^{-1} \hat{\mathbf{k}}^2 & m_{\text{LT}}^{-1} \hat{\mathbf{k}}_-^2 \\ m_{\text{LT}}^{-1} \hat{\mathbf{k}}_+^2 & m_*^{-1} \hat{\mathbf{k}}^2 \end{pmatrix}. \end{aligned} \quad (\text{A2})$$

Here the index  $i$  labels the particles,

$$m_*^{-1} = m^{-1} + m_{\text{LT}}^{-1},$$

where  $m$  is the particle mass,  $\hat{\mathbf{k}}_{\pm,i} = \hat{k}_{x,i} \pm i \hat{k}_{y,i}$ , and we have introduced  $\hat{\mathbf{K}} = \hat{\mathbf{k}}_1 + \hat{\mathbf{k}}_2$ ,  $\hat{\mathbf{K}}_{\pm} = \hat{\mathbf{k}}_{\pm,1} + \hat{\mathbf{k}}_{\pm,2}$ ,  $\hat{\mathbf{k}} = (\hat{\mathbf{k}}_1 - \hat{\mathbf{k}}_2)/2$ ,  $\hat{\mathbf{k}}_{\pm} = (\hat{\mathbf{k}}_{\pm,1} - \hat{\mathbf{k}}_{\pm,2})/2$ . The spin basis is  $|\uparrow\rangle$  and  $|\downarrow\rangle$ . The Hamiltonians of the type (A1) govern the dynamics of the lower exciton-polaritons in planar semiconductor microcavities. Derivation of a BCS-like Hamiltonian for the single-particle Hamiltonians (A1) will be presented below. The BCS-like pairing Hamiltonian for the  $\Omega$ -X-XX and  $\Omega$ -XX phases of excitons, which is of interest in this work, can be obtained along the same lines in the particular case of zero center-of-mass momentum of the pairs. The corresponding passage will be discussed at the end of this Appendix.

In the second quantization the general form of the pairing Hamiltonian reads

$$\hat{H} = \frac{1}{2} \sum_{\sigma_1 \sigma_2 \sigma_3 \sigma_4} \sum_{\mathbf{k}, \mathbf{K}, \mathbf{q}, \mathbf{Q}} \mathcal{H}_{\sigma_1 \sigma_2 \sigma_3 \sigma_4}^{k, \mathbf{K}, \mathbf{q}, \mathbf{Q}} \hat{C}_{\sigma_2 \sigma_1, \mathbf{q}, \mathbf{Q}}^{\dagger} \hat{C}_{\sigma_3 \sigma_4, \mathbf{k}, \mathbf{K}}, \quad (\text{A3})$$

where the pair annihilation operator  $\hat{C}_{\sigma \sigma', \mathbf{k}, \mathbf{K}}$  stands either for a pair of free particles with the same spin,  $\hat{C}_{\sigma \sigma, \mathbf{k}, \mathbf{K}} \equiv \hat{a}_{\sigma, -\mathbf{k} + \mathbf{K}/2} \hat{a}_{\sigma, \mathbf{k} + \mathbf{K}/2}$ , or for the molecular operator,  $\hat{C}_{\uparrow \downarrow, \mathbf{k}, \mathbf{K}} = \hat{C}_{\downarrow \uparrow, \mathbf{k}, \mathbf{K}} \equiv \hat{B}_{\mathbf{K}}$ . In the latter case the summation in (A3) over  $\mathbf{k}$  ( $\mathbf{q}$ ) is consistently absent. The matrix elements are defined as

$$\mathcal{H}_{\sigma_1 \sigma_2 \sigma_3 \sigma_4}^{k, \mathbf{K}, \mathbf{q}, \mathbf{Q}} = \int \psi_{\sigma_2 \sigma_1}^*(\mathbf{r}, \mathbf{R}) \hat{\mathcal{H}} \psi_{\sigma_3 \sigma_4}(\mathbf{r}, \mathbf{R}) d\mathbf{r} d\mathbf{R}, \quad (\text{A4})$$

with  $\mathbf{r} = \mathbf{r}_1 - \mathbf{r}_2$  and  $\mathbf{R} = (\mathbf{r}_1 + \mathbf{r}_2)/2$ . The wave functions are taken as

$$\psi_{\sigma \sigma}(\mathbf{r}, \mathbf{R}) = \frac{1}{S} e^{i\mathbf{k}\mathbf{r} + i\mathbf{K}\mathbf{R}} |\sigma \sigma\rangle \quad (\text{A5})$$

for free particles and

$$\psi_{\uparrow \downarrow}(\mathbf{r}, \mathbf{R}) = \frac{1}{\sqrt{S}} e^{i\mathbf{K}\mathbf{R}} \varphi_{\uparrow \downarrow}(\mathbf{r}) |\uparrow \downarrow\rangle \quad (\text{A6})$$

for the molecules. Here the function  $\varphi_{\uparrow \downarrow}(\mathbf{r})$  is a solution of the Schrodinger equation

$$\left( \frac{\hbar^2 \hat{\mathbf{k}}^2}{m_*} + V_{\uparrow \downarrow}(\mathbf{r}) \right) \varphi_{\uparrow \downarrow}(\mathbf{r}) = \varepsilon \varphi_{\uparrow \downarrow}(\mathbf{r}), \quad (\text{A7})$$

where the 2D potential  $V_{\uparrow \downarrow}(\mathbf{r})$  is assumed to be spherically symmetric. Upon substitution of

$$\varphi_{\uparrow \downarrow}(\mathbf{r}) = \frac{1}{\sqrt{S}} \sum_{\mathbf{k}} \phi_{\mathbf{k}} e^{i\mathbf{k}\mathbf{r}} \quad (\text{A8})$$

into Eq. (A7) one gets

$$\left(\varepsilon - \frac{\hbar^2 k^2}{m_*}\right)\phi_k = \frac{1}{S} \sum_q V_{\uparrow\downarrow}(\mathbf{q} - \mathbf{k})\phi_q, \quad (\text{A9})$$

which shows that *the phase* of the function  $\phi_k$  does not depend on  $k$ .

The operator  $\hat{\mathcal{H}}$  in Eq. (A4) is a sum of a free part constructed by the Kronecker summation of the single-particle Hamiltonians (A1) and the two-body interaction:

$$\hat{\mathcal{H}} = \hat{H}_1 \oplus \hat{H}_2 + \hat{\mathcal{V}}, \quad (\text{A10})$$

where

$$\hat{\mathcal{V}} = \begin{pmatrix} V_{\uparrow\uparrow}(\mathbf{r}) & 0 & 0 & 0 \\ 0 & V_{\uparrow\downarrow}(\mathbf{r}) & 0 & 0 \\ 0 & 0 & V_{\downarrow\uparrow}(\mathbf{r}) & 0 \\ 0 & 0 & 0 & V_{\downarrow\downarrow}(\mathbf{r}) \end{pmatrix}. \quad (\text{A11})$$

The diagonal contribution has three terms. The first one,

$$\frac{1}{2} \sum_{\sigma, k, \mathbf{K}} \left( \frac{\hbar^2 \mathbf{K}^2}{4m_*} + \frac{\hbar^2 k^2}{m_*} \right) \hat{C}_{\sigma\sigma, k, \mathbf{K}}^\dagger \hat{C}_{\sigma\sigma, k, \mathbf{K}},$$

is just the overall kinetic energy in a subsystem of free particles counted by pairs. This term can be recast in the standard

$$\frac{\hbar^2}{m_{\text{LT}}} \sum_{k, \mathbf{K}} \left[ \left( \frac{\mathbf{K}_-^2}{4} + k_-^2 \right) \phi_k \hat{B}_{\mathbf{K}} \hat{a}_{\uparrow, -k+\mathbf{K}/2}^\dagger \hat{a}_{\uparrow, k+\mathbf{K}/2}^\dagger + \left( \frac{\mathbf{K}_+^2}{4} + k_+^2 \right) \phi_k \hat{B}_{\mathbf{K}} \hat{a}_{\downarrow, -k+\mathbf{K}/2}^\dagger \hat{a}_{\downarrow, k+\mathbf{K}/2}^\dagger + \text{H.c.} \right].$$

The molecular condensate is characterized by macroscopic occupation of the molecular state with  $\mathbf{K} = 0$ . Following the Bogoliubov prescription, one may let  $\hat{B}_{\mathbf{K}} = \sqrt{N_{\text{B}}} \delta_{\mathbf{K}0}$ , where  $\delta_{\mathbf{K}0} = 1$  for  $\mathbf{K} = 0$  and  $\delta_{\mathbf{K}0} \equiv 0$  otherwise. One may then see that the pair coherence enhances dramatically the effective magnetic field due to the LT splitting. For large molecular occupation number  $N_{\text{B}} \gg 1$  one may have a sizable effect even for vanishingly small LT splitting of the single-particle states. The use of a single equation [(A7), where one may let  $m_* = m$ ] for the determination of the bound state energy and wave function is fully justified in this case.

Finally, we notice that the requirement for the single-particle Hamiltonians of the type (A1) to possess the property (A2) may be relaxed if, in considering the molecules, one limits oneself to only the  $\mathbf{K} = 0$  state. Thus, for a radiative doublet of excitons with  $k \gg q_0$ , where  $q_0$  is the boundary of the light cone, one may write

$$\begin{aligned} \hat{H} = & \sum_{\sigma, k} \left( \frac{\hbar^2 k^2}{2m} + \frac{\hbar v k}{2} \right) \hat{a}_{\sigma, k}^\dagger \hat{a}_{\sigma, k} + \frac{g}{2S} \sum_{k, q, \mathbf{K}, \sigma} \hat{a}_{\sigma, -q+\mathbf{K}/2}^\dagger \hat{a}_{\sigma, q+\mathbf{K}/2}^\dagger \hat{a}_{\sigma, -k+\mathbf{K}/2} \hat{a}_{\sigma, k+\mathbf{K}/2} \\ & + \varepsilon N_{\text{B}} + \hbar v \sqrt{N_{\text{B}}} \sum_k (k e^{-2i\varphi} \phi_k \hat{a}_{\uparrow, -k}^\dagger \hat{a}_{\uparrow, k}^\dagger + k e^{2i\varphi} \phi_k \hat{a}_{\downarrow, -k}^\dagger \hat{a}_{\downarrow, k}^\dagger + \text{H.c.}). \end{aligned} \quad (\text{A12})$$

Assuming  $\hbar v k \ll \varepsilon$ , one may omit the exchange term in the exciton kinetic energy and use Eq. (A7) (where one should let  $m_* = m$ ) for the calculation of  $\phi_k$ .

## APPENDIX B: CALCULATION OF THE PAIR-BREAKING EXCITATION SPECTRUM AND THE $\Omega$ -XX/ $\Omega$ -X-XX PHASE BOUNDARY

In the limit  $\beta \rightarrow 0$  the elementary excitation spectrum (13) takes the form

$$\varepsilon_p = \sqrt{\xi_p^2 - 4|\hbar\Omega_{\text{B}}^{(s)}(\mathbf{p}) \cdot \mathbf{S}_{\uparrow\downarrow}|^2}. \quad (\text{B1})$$

form

$$\sum_{\sigma, k} \frac{\hbar^2 k^2}{2m_*} \hat{a}_{\sigma, k}^\dagger \hat{a}_{\sigma, k}.$$

The second term is the two-body interaction between the particles with alike spins:

$$\frac{1}{2S} \sum_{k, q, \mathbf{K}, \sigma} \hat{a}_{\sigma, -q+\mathbf{K}/2}^\dagger \hat{a}_{\sigma, q+\mathbf{K}/2}^\dagger V_{\sigma\sigma}(\mathbf{k} - \mathbf{q}) \hat{a}_{\sigma, -k+\mathbf{K}/2} \hat{a}_{\sigma, k+\mathbf{K}/2}.$$

This term can be approximated by [53]

$$\frac{g}{2S} \sum_{k, q, \mathbf{K}, \sigma} \hat{a}_{\sigma, -q+\mathbf{K}/2}^\dagger \hat{a}_{\sigma, q+\mathbf{K}/2}^\dagger \hat{a}_{\sigma, -k+\mathbf{K}/2} \hat{a}_{\sigma, k+\mathbf{K}/2},$$

where  $g$  is the effective potential and we omit the momentum-dependent correction due to the dipolar tail of the bare potential assuming that this correction is small compared to the contact part. This excludes the dipolar-supersolid scenario from the consideration [30,31,61].

The last diagonal term

$$\sum_{\mathbf{K}} \left( \frac{\hbar^2 \mathbf{K}^2}{4m_*} + \varepsilon \right) \hat{B}_{\mathbf{K}}^\dagger \hat{B}_{\mathbf{K}}$$

is the energy of free molecules.

By collecting the off-diagonal terms one obtains

To obtain a consistent description in the vicinity of the scattering threshold  $|\varepsilon| \rightarrow 0$  where the molecular radius  $a_{\text{B}} = \sqrt{\hbar^2/m|\varepsilon|}$  diverges, one should account for the momentum dependence of the wave function  $\phi_p$ . For  $a_{\text{B}} \gg R_e$ , where  $R_e$  is the characteristic radius of the microscopic potential  $V_{\uparrow\downarrow}(r)$ , the normalized solution of the two-body problem (A7) takes the generic form

$$\varphi_{\uparrow\downarrow}(r) = \frac{1}{\sqrt{\pi a_{\text{B}}^2}} K_0(r/a_{\text{B}}), \quad (\text{B2})$$

where  $K_0(x)$  is the modified Bessel function of the second kind. This yields

$$\phi_p = \sqrt{\frac{4\pi}{S}} \frac{a_B}{1 + (pa_B)^2}. \quad (\text{B3})$$

This equation provides the proper behavior of the molecular exchange field equation (12) as a function of the density  $n_B$  to be employed in Eq. (B1). However, because of too cumbersome expressions produced by *Mathematica* in our attempt to find the minimum of Eq. (B1) with the ansatz (B3), we had to replace (B3) by a slightly modified form:

$$\phi_p = \sqrt{\frac{4\pi}{S}} \frac{a_B}{\sqrt{1 + (pa_B)^4}}. \quad (\text{B4})$$

We then verify *a posteriori* that (B3) yields quantitatively similar results [by direct evaluation of Eq. (B1) at several points once the approximate location of the phase boundary has been worked out using Eq. (B4)].

By substituting Eq. (12) with  $\phi_p$  given by (B4) and Eq. (11) with  $n_B = (2\mu - \varepsilon)/g_B$  (see Sec. III), one gets

$$\begin{aligned} & \varepsilon_p^{(\nu, \sigma)}(E_p, \mu, \varepsilon) \\ &= \sqrt{\left(\frac{E_p}{2} + \frac{\sigma\mu - \varepsilon}{2 - \sigma}\right)^2 - \frac{2\nu(2\mu - \varepsilon)E_p}{2 - \sigma} \frac{1}{|\varepsilon|} \left(1 + \frac{E_p}{|\varepsilon|}\right)^{-2}}, \end{aligned} \quad (\text{B5})$$

where  $E_p = \hbar^2 p^2/m$  and we have defined

$$\nu = \frac{8\pi \hbar^2 \nu^2}{g_{XB}} \quad (\text{B6})$$

and

$$\sigma = 2 - \frac{g_B}{g_{XB}}. \quad (\text{B7})$$

We have omitted the exchange term  $\hbar\nu p/2$  assuming it is small compared to  $\varepsilon$ . This assumption is justified for dipolar excitons characterized by a relatively long lifetime  $\tau$ . The minimum  $E_\Omega(\mu, \varepsilon)$  of the function (B5) is then represented by the unique real root of a quintic polynomial. We substitute  $E_\Omega(\mu, \varepsilon)$  back into (B5) to get a family of functions  $\varepsilon_\Omega^{(\nu, \sigma)}(\varepsilon, \mu) \equiv \varepsilon_p^{(\nu, \sigma)}[E_\Omega(\mu, \varepsilon), \mu, \varepsilon]$  defined on the plane  $\mu$  versus  $\varepsilon$ . We then graphically obtain solutions of  $\varepsilon_\Omega^{(\nu, \sigma)}(\varepsilon, \mu) = 0$  in this plane.

The solution used to trace the  $\Omega$ -XX/ $\Omega$ -X-XX boundary in Fig. 3 has been obtained for  $\nu = 10$  (in units of  $\hbar^2 q_0^2/m$ ) and  $\sigma = 1$ . This value of  $\nu$  can be realized, e.g., with  $\tau = 100$  ps and  $g_{XB} = \tilde{g}\hbar^2/m$ , where  $m$  is the exciton mass in MoS<sub>2</sub>

and  $\tilde{g} = 1$ . The known value of the bright exciton lifetime in a *monolayer* of MoS<sub>2</sub> amounts to several picoseconds [37]. It is quite plausible that this value may be increased by two orders of magnitude when going to a homobilayer structure. The choice  $\tilde{g} \sim 1$  is justified *a posteriori* by evaluating the well-known expression  $\tilde{g} = 4\pi/\ln(E_a/2\mu)$  for the relevant values of  $\mu$  in Fig. 3. Here  $E_a = \hbar^2/ma^2$ , with  $a$  being on the order of  $a_X$  (see, e.g., Ref. [53] and references therein). The interaction constant  $g_X$  is assumed such that the first-order ray anticipated in Sec. III falls into the area occupied by the  $\Omega$ -X-XX phase in Fig. 3 and, consequently, is irrelevant. Finally, by using the relation  $n_B = (2\mu - \varepsilon)/g_B$  one can estimate  $n_B \sim 10^{11}$  cm<sup>-2</sup> for the biexciton density at the  $\Omega$ -XX/ $\Omega$ -X-XX phase boundary.

### APPENDIX C: THE PERIOD OF THE EXCITON STRIPES IN THE $\Omega$ -X-XX PHASE

The energy density of the  $\Omega$ -X-XX phase reads

$$\begin{aligned} \frac{E_{\Omega-X-XX}}{S} &= \left( \xi_q - \sqrt{\frac{\hbar^2 n_B \beta}{2\pi m}} - 2|\hbar\Omega_B^{(s)}(\mathbf{q}) \cdot \mathbf{S}_{\uparrow\downarrow}| \right) |\Psi_X|^2 \\ &+ 4g_X |\Psi_X|^4 + \frac{E_B}{S}, \end{aligned} \quad (\text{C1})$$

where  $E_B$  is given by Eq. (10). Minimization with respect to  $q$  yields Eq. (14). Neglecting the  $\nu/2$  term and using the ansatz (B4), one gets (in the notations adopted in Appendix B)

$$\frac{\partial}{\partial E_q} \sqrt{\frac{\nu(2\mu - \varepsilon)E_q}{2(2 - \sigma)|\varepsilon|(1 + E_q^2/\varepsilon^2)}} = \frac{1}{4}. \quad (\text{C2})$$

By introducing  $x \equiv E_q/|\varepsilon|$  one may reduce this equation to

$$\frac{\partial}{\partial x} \sqrt{\frac{x}{1 + x^2}} = \frac{1}{4} f(\mu, \varepsilon), \quad (\text{C3})$$

where

$$f(\mu, \varepsilon) \equiv |\varepsilon| \sqrt{\frac{2(2 - \sigma)}{\nu(2\mu - \varepsilon)}} \quad (\text{C4})$$

is a monotonously decreasing function of the chemical potential  $\mu$ . One can see that  $x = 1$  at  $f = 0$  and  $x \rightarrow 0$  at  $f \rightarrow +\infty$ . The asymptotic solution  $x \rightarrow 0$  at  $2\mu \rightarrow \varepsilon + 0$  defines the boundary with the radiative X-XX phase (light gray area on the phase diagram shown in Fig. 3).

[1] E. Hanamura and H. Haug, *Phys. Rep.* **33**, 209 (1977).  
 [2] S. Moskalenko, *Zh. Opt. Spektrosk.* **5**, 147 (1958).  
 [3] M. A. Lampert, *Phys. Rev. Lett.* **1**, 450 (1958).  
 [4] A. Mysyrowicz, J. Grun, R. Levy, A. Bivas, and S. Nikitine, *Phys. Lett. A* **26**, 615 (1968).  
 [5] V. Agranovich, N. Efremov, and H. Kaminskaya, *Opt. Commun.* **3**, 387 (1971).

[6] W. F. Brinkman, T. M. Rice, and B. Bell, *Phys. Rev. B* **8**, 1570 (1973).  
 [7] V. D. Kulakovskii, V. G. Lysenko, and V. B. Timofeev, *Phys. Usp.* **28**, 735 (1985).  
 [8] P. Nozières and D. Saint James, *J. Phys. (Paris)* **43**, 1133 (1982).  
 [9] R. C. Miller, D. A. Kleinman, A. C. Gossard, and O. Munteanu, *Phys. Rev. B* **25**, 6545 (1982).



- [10] J. C. Kim and J. P. Wolfe, *Phys. Rev. B* **57**, 9861 (1998).
- [11] R. Spiegel, G. Bacher, A. Forchel, B. Jobst, D. Hommel, and G. Landwehr, *Phys. Rev. B* **55**, 9866 (1997).
- [12] Y. You, X.-X. Zhang, T. C. Berkelbach, M. S. Hybertsen, D. R. Reichman, and T. F. Heinz, *Nat. Phys.* **11**, 477 (2015).
- [13] Z. Ye, L. Waldecker, E. Y. Ma, D. Rhodes, A. Antony, B. Kim, X.-X. Zhang, M. Deng, Y. Jiang, Z. Lu, D. Smirnov, K. Watanabe, T. Taniguchi, J. Hone, and T. F. Heinz, *Nat. Commun.* **9**, 3718 (2018).
- [14] Z. Li, T. Wang, Z. Lu, C. Jin, Y. Chen, Y. Meng, Z. Lian, T. Taniguchi, K. Watanabe, S. Zhang, D. Smirnov, and S.-F. Shi, *Nat. Commun.* **9**, 3719 (2018).
- [15] M. Kremser, M. Brotons-Gisbert, J. Knörzer, J. Gückelhorn, M. Meyer, M. Barbone, A. V. Stier, B. D. Gerardot, K. Müller, and J. J. Finley, *npj 2D Mater. Appl.* **4**, 8 (2020).
- [16] W. Li, X. Lu, S. Dubey, L. Devenica, and A. Srivastava, *Nat. Mater.* **19**, 624 (2020).
- [17] A. V. Larionov, V. B. Timofeev, P. A. Ni, S. V. Dubonos, I. Hvam, and K. Soerensen, *J. Exp. Theor. Phys. Lett.* **75**, 570 (2002).
- [18] A. A. High, J. R. Leonard, A. T. Hammack, M. M. Fogler, L. V. Butov, A. V. Kavokin, K. L. Campman, and A. C. Gossard, *Nature (London)* **483**, 584 (2012).
- [19] R. Anankine, M. Beian, S. Dang, M. Alloing, E. Cambri, K. Merghem, C. G. Carbonell, A. Lemaître, and F. Dubin, *Phys. Rev. Lett.* **118**, 127402 (2017).
- [20] K. Cohen, Y. Shilo, K. West, L. Pfeiffer, and R. Rapaport, *Nano Lett.* **16**, 3726 (2016).
- [21] S. Misra, M. Stern, A. Joshua, V. Umansky, and I. Bar-Joseph, *Phys. Rev. Lett.* **120**, 047402 (2018).
- [22] M. Stern, V. Umansky, and I. Bar-Joseph, *Science* **343**, 55 (2014).
- [23] Y. Mazuz-Harpaz, K. Cohen, M. Leveson, K. West, L. Pfeiffer, M. Khodas, and R. Rapaport, *Proc. Natl. Acad. Sci. USA* **116**, 18328 (2019).
- [24] M. M. Fogler, L. V. Butov, and K. S. Novoselov, *Nat. Commun.* **5**, 4555 (2014).
- [25] P. Rivera, J. R. Schaibley, A. M. Jones, J. S. Ross, S. Wu, G. Aivazian, P. Klement, K. Seyler, G. Clark, N. J. Ghimire, J. Yan, D. G. Mandrus, W. Yao, and X. Xu, *Nat. Commun.* **6**, 6242 (2015).
- [26] S. Dang, M. Zamorano, S. Suffit, K. West, K. Baldwin, L. Pfeiffer, M. Holzmann, and F. Dubin, *Phys. Rev. Research* **2**, 032013(R) (2020).
- [27] G. Wang, A. Chernikov, M. M. Glazov, T. F. Heinz, X. Marie, T. Amand, and B. Urbaszek, *Rev. Mod. Phys.* **90**, 021001 (2018).
- [28] C. Schindler and R. Zimmermann, *Phys. Rev. B* **78**, 045313 (2008).
- [29] A. D. Meyertholen and M. M. Fogler, *Phys. Rev. B* **78**, 235307 (2008).
- [30] S. V. Andreev, *Phys. Rev. B* **92**, 041117(R) (2015).
- [31] S. V. Andreev, *Phys. Rev. B* **94**, 140501(R) (2016).
- [32] Dipolar biexcitons with positive energies were recently observed in 2D traps [15,16]. However, if the confinement length approaches the exciton Bohr radius, the biexciton binding energy may become negative even in the case where electrons and holes reside in the same layer [Al. L. Efros and A. V. Rodina, *Solid State Commun.* **72**, 645 (1989); A. A. Golovatenko, M. A. Semina, A. V. Rodina, and T. V. Shubina, *Phys. Solid State* **59**, 1215 (2017)]. Which of the two effects is responsible for the experimental findings [15,16] remains to be understood.
- [33] D. S. Citrin, *Phys. Rev. B* **50**, 17655 (1994).
- [34] G. E. Pikus and G. L. Bir, *Sov. Phys. JETP* **33**, 195 (1970).
- [35] M. Z. Maialle, E. A. de Andrada e Silva, and L. J. Sham, *Phys. Rev. B* **47**, 15776 (1993).
- [36] S. V. Gupalov, E. L. Ivchenko, and A. V. Kavokin, *J. Exp. Theor. Phys.* **86**, 388 (1998).
- [37] M. M. Glazov, T. Amand, X. Marie, D. Lagarde, L. Bouet, and B. Urbaszek, *Phys. Rev. B* **89**, 201302(R) (2014).
- [38] G. Dresselhaus, *Phys. Rev.* **100**, 580 (1955).
- [39] Y. A. Bychkov and E. I. Rashba, *J. Phys. C* **17**, 6039 (1984).
- [40] M. I. Dyakonov and V. Y. Kachorovskii, *Sov. Phys. Semicond.* **20**, 110 (1986).
- [41] T. D. Stanescu, B. Anderson, and V. Galitski, *Phys. Rev. A* **78**, 023616 (2008).
- [42] S. V. Andreev and A. V. Nalitov, *Phys. Rev. B* **97**, 165139 (2018).
- [43] C.-J. Wu, I. Mondragon-Shem, and X.-F. Zhou, *Chin. Phys. Lett.* **28**, 097102 (2011).
- [44] Y. Li, L. P. Pitaevskii, and S. Stringari, *Phys. Rev. Lett.* **108**, 225301 (2012).
- [45] J.-R. Li, J. Lee, W. Huang, S. Burchesky, B. Shteynas, F. Ç. Top, A. O. Jamison, and W. Ketterle, *Nature (London)* **543**, 91 (2017).
- [46] A. Putra, F. Salces-Cárcoba, Y. Yue, S. Sugawa, and I. B. Spielman, *Phys. Rev. Lett.* **124**, 053605 (2020).
- [47] A. J. Leggett, in *Modern Trends in the Theory of Condensed Matter*, edited by A. Pełalski and J. A. Przystawa (Springer, Berlin, 1980), pp. 13–27.
- [48] V. Gurarie and L. Radzihovsky, *Ann. Phys. (NY)* **322**, 2 (2007).
- [49] R. Hanai, P. B. Littlewood, and Y. Ohashi, *Phys. Rev. B* **96**, 125206 (2017).
- [50] M. W. J. Romans, R. A. Duine, S. Sachdev, and H. T. C. Stoof, *Phys. Rev. Lett.* **93**, 020405 (2004).
- [51] L. Radzihovsky, J. Park, and P. B. Weichman, *Phys. Rev. Lett.* **92**, 160402 (2004).
- [52] L. Radzihovsky, P. B. Weichman, and J. I. Park, *Ann. Phys. (NY)* **323**, 2376 (2008).
- [53] O. I. Utesov, M. I. Baglay, and S. V. Andreev, *Phys. Rev. A* **97**, 053617 (2018).
- [54] A. I. Safonov, S. A. Vasilyev, I. S. Yasnikov, I. I. Lukashevich, and S. Jaakkola, *Phys. Rev. Lett.* **81**, 4545 (1998).
- [55] R. Desbuquois, L. Chomaz, T. Yefsah, J. Léonard, J. Beugnon, C. Weitenberg, and J. Dalibard, *Nat. Phys.* **8**, 645 (2012).
- [56] S. V. Andreev, *Phys. Rev. B* **95**, 184519 (2017).
- [57] L. Santos, G. V. Shlyapnikov, and M. Lewenstein, *Phys. Rev. Lett.* **90**, 250403 (2003).
- [58] A. Filinov, N. V. Prokof'ev, and M. Bonitz, *Phys. Rev. Lett.* **105**, 070401 (2010).
- [59] O. L. Berman, Y. E. Lozovik, D. W. Snoke, and R. D. Coalson, *Phys. Rev. B* **70**, 235310 (2004).
- [60] G. E. Astrakharchik, J. Boronat, I. L. Kurbakov, and Y. E. Lozovik, *Phys. Rev. Lett.* **98**, 060405 (2007).
- [61] D. V. Fil and S. I. Shevchenko, *Low Temp. Phys.* **42**, 794 (2016).
- [62] R. A. Suris, *J. Exp. Theor. Phys.* **122**, 602 (2016).

- [63] A. M. Polyakov, *Phys. Lett. B* **59**, 79 (1975).
- [64] This is in qualitative analogy to the destabilization of a unidirectional Larkin-Ovchinnikov state by fluctuations studied in L. Radzihovsky and A. Vishwanath, *Phys. Rev. Lett.* **103**, 010404 (2009).
- [65] J. Toner and D. R. Nelson, *Phys. Rev. B* **23**, 316 (1981).
- [66] G. Panzarini, L. C. Andreani, A. Armitage, D. Baxter, M. S. Skolnick, V. N. Astratov, J. S. Roberts, A. V. Kavokin, M. R. Vladimirova, and M. A. Kaliteevski, *Phys. Rev. B* **59**, 5082 (1999).
- [67] A. Kavokin, G. Malpuech, and M. Glazov, *Phys. Rev. Lett.* **95**, 136601 (2005).
- [68] O. Bleu, D. D. Solnyshkov, and G. Malpuech, *Phys. Rev. B* **96**, 165432 (2017).
- [69] Z. Zhang, L. Chen, K.-X. Yao, and C. Chin, *Nature* **592**, 708 (2021).
- [70] J. Ruseckas, G. Juzeliūnas, P. Öhberg, and M. Fleischhauer, *Phys. Rev. Lett.* **95**, 010404 (2005).
- [71] J. Dalibard, F. Gerbier, G. Juzeliūnas, and P. Öhberg, *Rev. Mod. Phys.* **83**, 1523 (2011).